

# Metabolomic biomarkers of acute radiation syndrome and delayed effects of acute radiation exposure : correlation with histological and clinical endpoints

Swarnima Pandey<sup>1</sup>, Nageswara Pilli<sup>1</sup>, Praveen Kumar<sup>1</sup>, Jace W. Jones<sup>1</sup>, George Parker<sup>2</sup>, Gregory Tudor<sup>3</sup>, Catherine Booth<sup>3</sup>, Ann M. Farese<sup>4</sup>, Thomas J. MacVittie<sup>4</sup>, Polly Chang<sup>5</sup>, Maureen A Kane<sup>1</sup>

<sup>1</sup> University of Maryland, School of Pharmacy, Department of Pharmaceutical Sciences, <sup>2</sup> Charles River, <sup>3</sup> Epistem Ltd., Manchester, UK, <sup>4</sup> University of Maryland, School of Medicine, Department of Radiation Oncology, <sup>5</sup> SRI, International

## INTRODUCTION

Exposure to high dose irradiation following a nuclear or radiological incident will result in the acute radiation syndrome (ARS) of the gastrointestinal (GI-ARS) system in a dose- and time-dependent manner, which will be followed by delayed effects of acute radiation exposure (DEARE)

Using validated models of partial body irradiation with bone marrow sparing, large-scale, longitudinal, targeted metabolomic profiling was conducted across multiple studies to identify biomarkers of radiation-induced injury using liquid chromatography-tandem mass spectrometry-based analyses of plasma, as well as select tissues and then correlative analyses was performed with survival and/or histological endpoints using Pearson's r.

Correlation with clinical and/or histological endpoints defines the context of use and provides an opportunity for biomarker use in the development of medical countermeasures

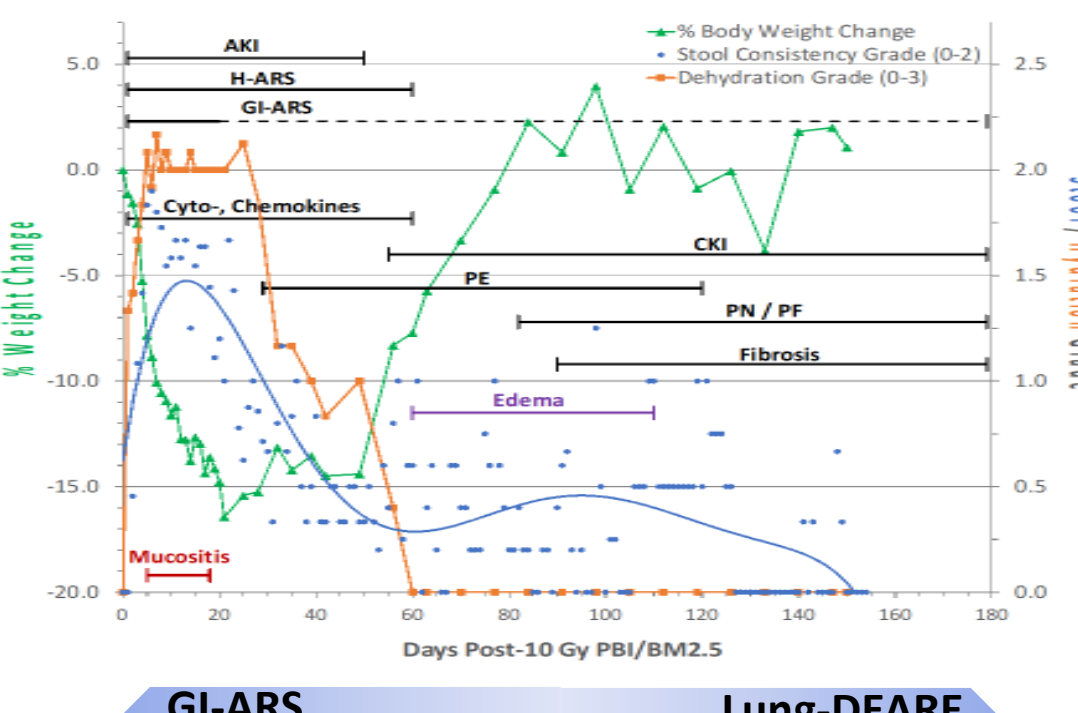


**Figure 1. Radiation-induced injury as a function of time:** The multi-organ injury within the ARS and DEARE and clinical signs for NHP consequent to 10 Gy PBI/BM2.5 [1-3]

## METHODS & STUDIES

### A. Study Design

Non-human primates consisted of male rhesus macaques (*Macaca mulatta*) that were exposed to radiation doses between 10 to 12 Gy of partial body irradiation with either 2.5% or 5% bone marrow sparing (PBI/BM5 or PBI/BM2.5) with a peak 6MV linear accelerator (LINAC)-derived photons with an average energy of 2 MV at 0.80 Gy min<sup>-1</sup>. Bone marrow sparing was accomplished with tibiae outside the beam field. Description of the animal models, including radiation exposure and dosimetry, medical management (supportive care and health monitoring), as well as collection of plasma and tissue, have been described previously [1-4]. Plasma and tissue were frozen upon collection, and stored at -80C until assay.

| Study | Radiation Dose | Exposure  | Matrix | ImmPort Accession Number |
|-------|----------------|-----------|--------|--------------------------|
| AXR16 | 10, 11, 12 Gy  | PBI/BM5   | Plasma | SDY1997                  |
| AXR23 | 10 Gy          | PBI/BM5   | Plasma | SDY1854                  |
| AXR24 | 10 Gy          | PBI/BM2.5 | Plasma | SDY2058                  |
| AXR26 | 12 Gy          | PBI/BM2.5 | Plasma | SDY2002                  |

A summary of the studies included in the biomarker analyses is in **Table 1**.

\* ImmPort is funded by the NIH, NIAID and DAIT in support of the NIH mission to share data with the public.

**Table 1. Studies included in biomarker analyses.** The data supporting this poster is available at ImmPort\* (<https://www.immport.org>) under the following study accession numbers.

### B. Biomarker Quantification

Plasma (and tissue) were analyzed for their metabolomic signature using a liquid chromatography-tandem mass spectrometry (LC-MS/MS)-based targeted metabolomics workflow that we have described in detail previously [6-10].

**LC-MS/MS.** Targeted, quantitative metabolomics was performed using Biocrates AbsoluteIDQ p180, MxP Quant 500, or MxP Quant 500 XL kit (Biocrates, Life Science AG, Innsbruck, Austria). Metabolite detection is done via pre-selected reaction monitoring (SRM) transitions on a tandem mass spectrometry platform that consisted of an ACQUITY I-Class UPLC coupled to a Xevo TQ-S or Xevo TQ-XS tandem quadrupole mass spectrometer (Waters Corporation, Milford, MA).

**Data analysis.** MetIQ software (Biocrates) controlled the assay workflow including sample registration, calculation of metabolite concentrations, and assay validation. The data generated from the Biocrates kit, which included analyte name and calculated concentration, were imported into MetaboAnalyst for multivariate analysis. Statistical analyses were performed using the MetaboAnalyst 5.0 web-based statistical package and GraphPad Prism (v 7.03, La Jolla, CA).

### C. Histological Scoring

#### GI-ARS

Corrected crypt number as an index of crypt survival was measured as described previously [2]. Samples of small intestine were collected at necropsy and fixed in formalin, embedded in paraffin, cut and mounted, and stained with hematoxylin and eosin (H&E). The number of surviving and regenerating crypts per length of intestine was scored, and the average per group was calculated. The size of surviving crypts varied, which influenced the likelihood of surviving crypt in cross section, so a size correction factor was applied to reduce this error based on widths of crypts in nonirradiated control NHPs and surviving crypts in irradiated NHPs. The corrected number of crypts was calculated according to the following equation: corrected number of crypts = (mean width in control/mean width in irradiated) x mean number of surviving crypts in the irradiated.

#### Lung-DEARE.

Sixteen different histological assessments (**Table 2**) were made by George Parker as part of the studies listed in **Table 1**. Histological assessment is described in detail in [5] and data will be available from ImmPort (**Table 1**).

**Table 2. Histological endpoints assessed for lung-DEARE**

| Histological Endpoints Assessed in Lung           |  |
|---|--|
| CTGF-positive staining, alveolus/duct             |  |
| CTGF-positive staining, pleural                   |  |
| CTGF-positive staining, interstitial              |  |
| Collagen-1 IHC interstitial/increased staining    |  |
| Collagen-1 IHC pleural surface/increased staining |  |
| MPO IHC-pos. staining                             |  |
| CD206-alveolar macrophages                        |  |
| CD163-alveolar macrophages                        |  |
| CD163-interstitial macrophages                    |  |
| Congestion  |  |
| Edema, alveolar                                   |  |
| Inflammation, interstitial                        |  |
| Infiltration, lymphocytic                         |  |
| Infiltration, neutrophilic                        |  |
| Accumulation, alv macrophages                     |  |
| Trichrome-fibrosis, interstitial                  |  |

## BIOMARKER CORRELATION WITH CLINICAL OUTCOME AND HISTOLOGICAL ASSESSMENTS

### A. ACUTE RADIATION SYNDROME : BIOMARKERS FOR GI ARS

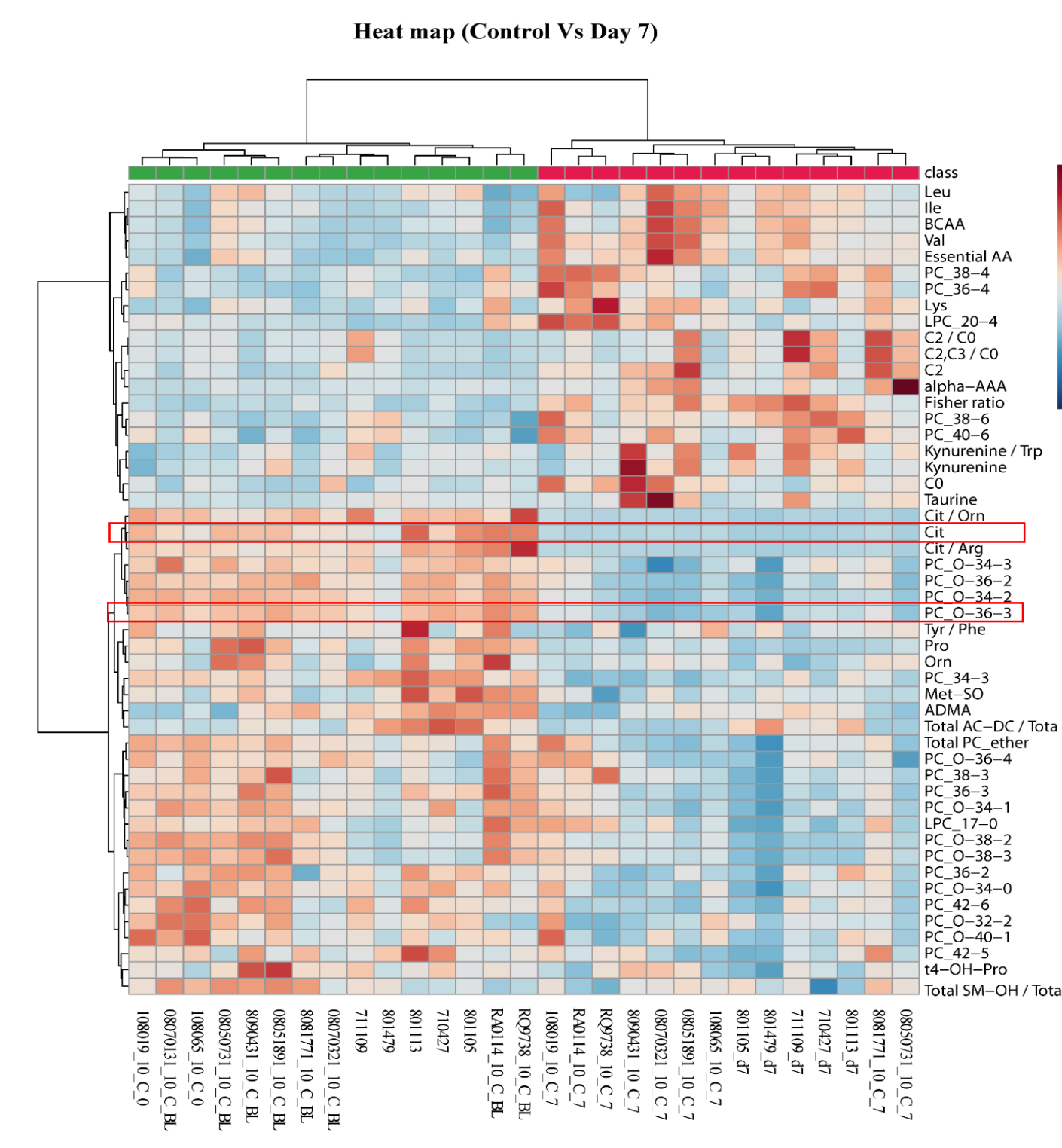


**Figure 2: Plasma metabolomic profile during GI-ARS.** Hierarchical clustering displays statistical metabolite differences between non-irradiated NHP (control/naïve) and Irradiated (D7). Heatmap displaying the top 50 metabolites based on t-test/ANOVA, Euclidean distancing, and Ward clustering, comparing metabolite profiles at (a) control (green) and D7 (red). D7 irradiated data is from AXR23, n=5; AXR24, n=10 (n=15 total D7 irradiated). Unirradiated / naïve, n=14. (10 Gy PBI/BM5 (AXR23) or 10 Gy PBI/BM2.5 (AXR24)).

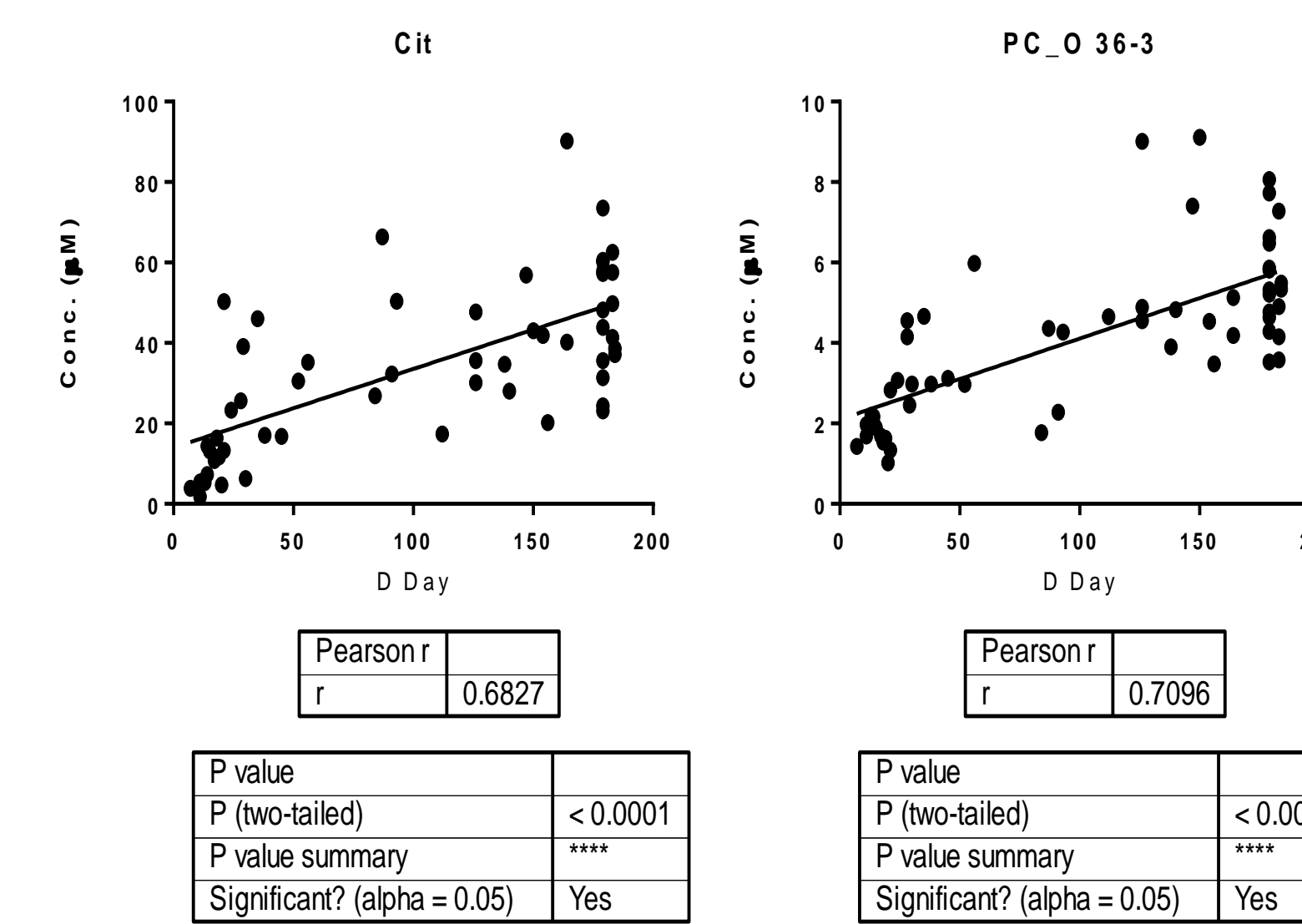
Biomarkers boxed in red have correlation with survival (**Table 3, Figure 3**) and correlation with histological endpoints (**Table 4, Figure 4**) shown as representative examples.

#### Correlation of GI-ARS candidate plasma biomarkers with survival

| Metabolites  | r     | p value |
|--------------|-------|---------|
| PC_36-3      | 0.73  | <0.0001 |
| PC_O-36-3    | 0.7   | <0.0001 |
| Cit          | 0.68  | <0.0001 |
| PC_34-3      | 0.64  | <0.0001 |
| PC_O-36-2    | 0.61  | <0.0001 |
| Cit/Arg      | 0.59  | <0.0001 |
| Cit/Orn      | 0.59  | <0.0001 |
| PC_36-2      | 0.57  | <0.0001 |
| PC_O-32-2    | 0.52  | <0.0001 |
| Tyr/Phe      | 0.44  | 0.005   |
| PC_O-38-3    | 0.36  | 0.005   |
| PC_42-6      | 0.36  | 0.005   |
| PC_O-38-2    | 0.31  | 0.01    |
| Met SO4      | 0.31  | 0.01    |
| PC_38-6      | -0.31 | 0.01    |
| BCAA         | -0.36 | 0.004   |
| Fisher ratio | -0.53 | <0.0001 |

**Table 3: Correlation between candidate metabolomic biomarkers for GI-ARS and survival.** List of significant metabolites illustrating their Pearson's correlation (r) with survival. Highlighted in red are representative examples for which correlation plots are shown in **Figure 3**. Data used for correlative analysis was from plasma analysis of AXR23, n=20; AXR24, n=38 (10 Gy PBI/BM5 (AXR23) or 10 Gy PBI/BM2.5 (AXR24)).

### CORRELATION WITH SURVIVAL



| P value                     | < 0.0001 |
|-----------------------------|----------|
| P (two-tailed)              | ****     |
| P value summary             | ****     |
| Significant? (alpha = 0.05) | Yes      |

| P value                     | < 0.0001 |
|-----------------------------|----------|
| P (two-tailed)              | ****     |
| P value summary             | ****     |
| Significant? (alpha = 0.05) | Yes      |

### CORRELATION WITH HISTOLOGICAL ENDPOINTS

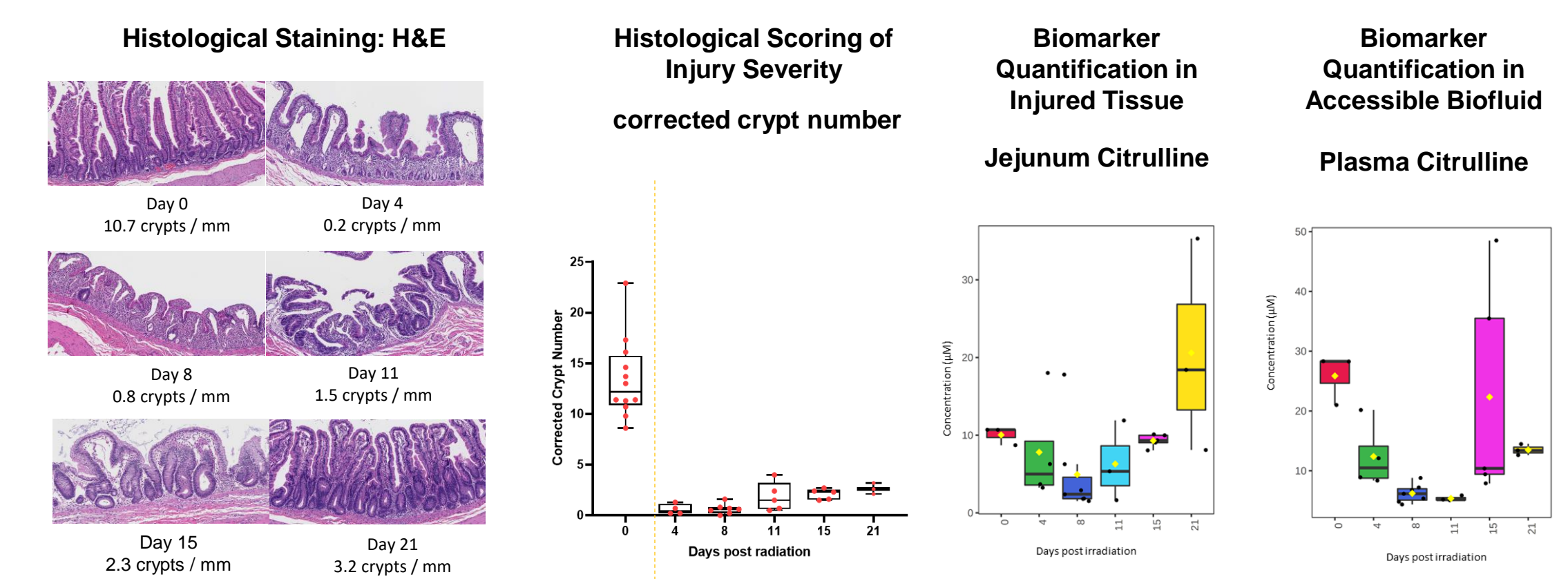


**Figure 4: Histological scoring of endpoints and quantification of candidate metabolomic biomarkers for GI-ARS.** Representative images of H&E staining used in scoring to determine corrected crypt number. Correlation plots from **Table X** which lists significant metabolites and their Pearson's correlation (r) with survival. Data used for correlative analysis was from plasma analysis of AXR26, n=24 (12 Gy PBI/BM2.5).

#### A. Jejunum – CCN correlation

| Analyte           | R    | p-value |
|-------------------|------|---------|
| PC ae C36:2       | 0.62 | 0.0010  |
| PC ae C38:1       | 0.60 | 0.0015  |
| PC ae C38:2       | 0.52 | 0.0073  |
| PC ae C34:3       | 0.35 | 0.0902  |
| PC ae C34:2       | 0.66 | 0.0004  |
| Serotonin         | 0.42 | 0.0344  |
| Acylcarnitine C18 | 0.30 | 0.1451  |
| PC ae C36:3       | 0.76 | <0.0001 |
| Citrulline        | 0.54 | 0.0051  |

#### B. Plasma – CCN correlation

| Analyte           | R     | p-value |
|-------------------|-------|---------|
| PC ae C36:2       | 0.18  | 0.3850  |
| PC ae C38:1       | 0.11  | 0.6119  |
| PC ae C38:2       | 0.20  | 0.3481  |
| PC ae C34:3       | 0.35  | 0.0839  |
| PC ae C34:2       | 0.23  | 0.2783  |
| Serotonin         | -0.07 | 0.7532  |
| Acylcarnitine C18 | 0.05  | 0.7965  |
| PC ae C36:3       | 0.28  | 0.1747  |
| Citrulline        | 0.67  | 0.0003  |

**Table 4. Correlation between candidate metabolomic biomarkers for GI-ARS and histological scoring for corrected crypt number (CCN).** List of significant metabolites illustrating their Pearson's correlation (r) with CCN in either (A.) jejunum or (B.) plasma. Biomarker data used for correlative analysis was from plasma or jejunum from AXR26, n=24 (12 Gy PBI/BM2.5).

## B. DELAYED EFFECT OF RADIATION EXPOSURE: ACUTE RADIATION SYNDROME : BIOMARKERS FOR LUNG DEARE

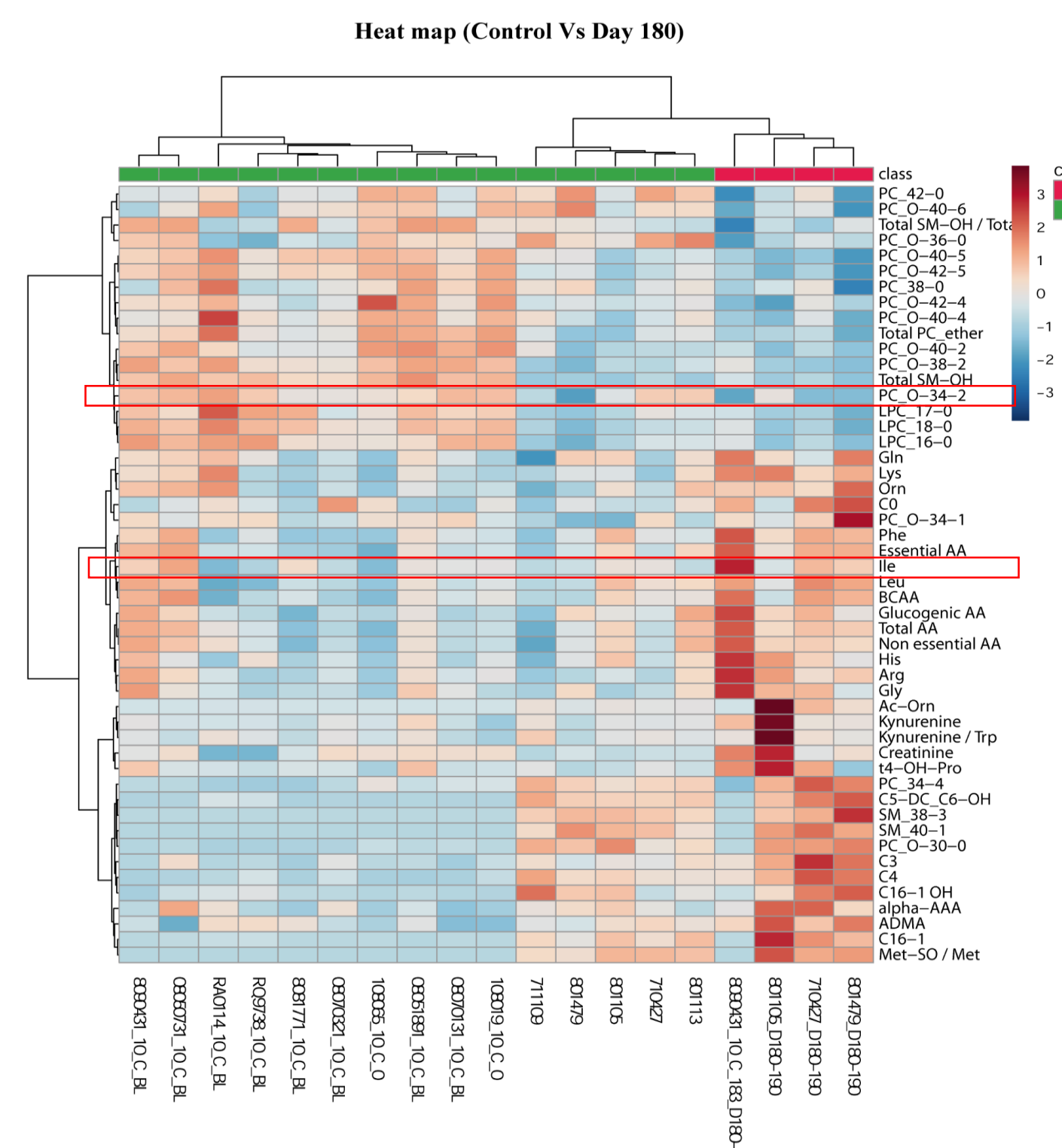


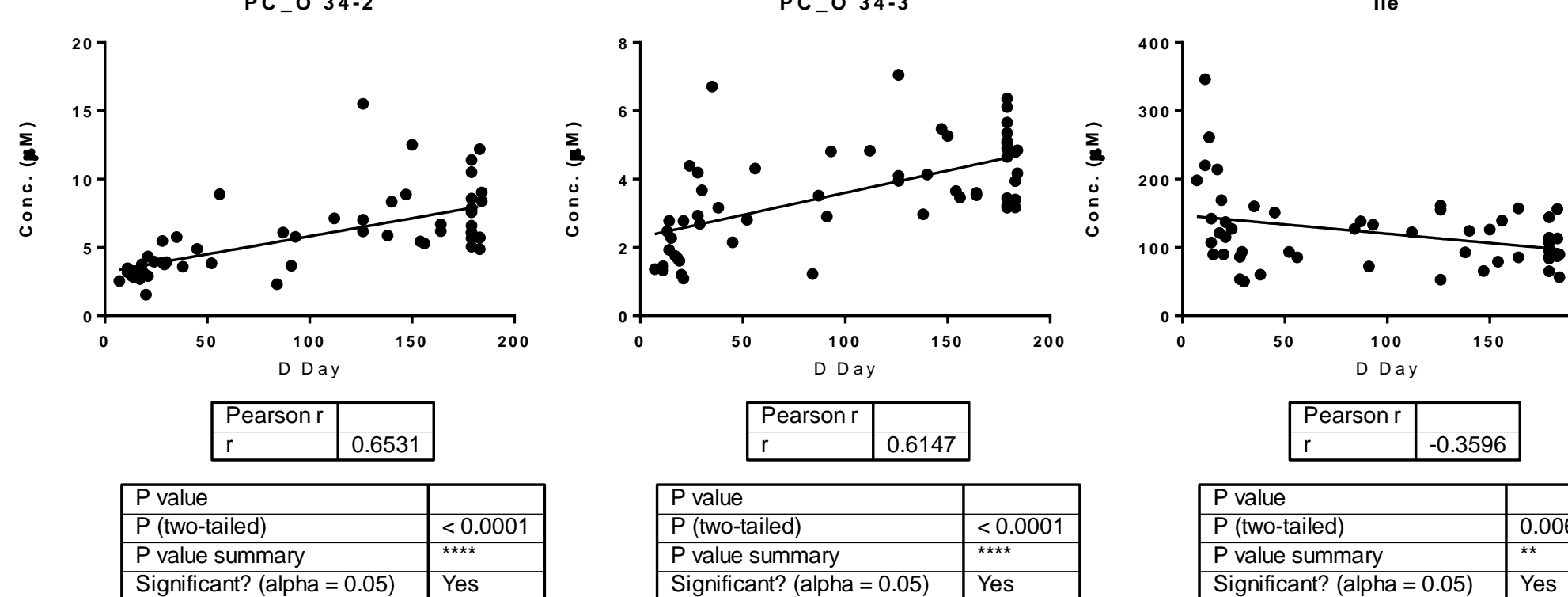
**Figure 5: Plasma metabolomic profile during Lung-DEARE.** Hierarchical clustering displays statistical metabolite differences between non-irradiated NHP (control) and Irradiated (D180): control and Day 180 (D180). Heatmap displaying the top 50 metabolites based on t-test/ANOVA, Euclidean distancing, and Ward clustering, comparing metabolite profiles at (a) control (green) and D180 (red). D180 irradiated data is from AXR23, n=1; AXR24, n=3 (n=4 total D180 irradiated). Unirradiated / naïve, n=15. (10 Gy PBI/BM5 (AXR23) or 10 Gy PBI/BM2.5 (AXR24)).

#### Correlation of lung-DEARE candidate plasma biomarkers with survival

| Metabolites | r     | p value |
|-------------|-------|---------|
| PC_O-34-2   | 0.65  | <0.0001 |
| PC_O-34-3   | 0.61  | <0.0001 |
| PC_42-0     | 0.39  | 0.002   |
| PC_O-36-0   | 0.36  | 0.004   |
| Gln         | 0.31  | 0.01    |
| PC_O-42-5   | 0.28  | 0.03    |
| Ile         | -0.35 | 0.006   |

**Table 5: Correlation between candidate metabolomic biomarkers for Lung-DEARE and survival.** List of significant metabolites illustrating their Pearson's correlation (r) with survival. Highlighted in red are representative examples for which correlation plots are shown in **Figure 6**. Data used for correlative analysis was from plasma analysis of AXR23, n=20; AXR24, n=38 (10 Gy PBI/BM5 (AXR23) or 10 Gy PBI/BM2.5 (AXR24)).

### CORRELATION WITH SURVIVAL



| P value                     | < 0.0001 |
|-----------------------------|----------|
| P (two-tailed)              | ****     |
| P value summary             | ****     |
| Significant? (alpha = 0.05) | Yes      |

| P value                     | < 0.0001 |
|-----------------------------|----------|
| P (two-tailed)              | ****     |
| P value summary             | ****     |
| Significant? (alpha = 0.05) | Yes      |

| P value                     | 0.0060 |
|-----------------------------|--------|
| P (two-tailed)              | **     |
| P value summary             | **     |
| Significant? (alpha = 0.05) | Yes    |

### CORRELATION WITH HISTOLOGICAL ENDPOINTS

| Biomarker | TGFB-positive staining, interstitial | Collagen-1 IHC pleural surface/increased staining | Edema, alveolar               | Trichrome-fibrosis, interstitial | Infiltration, neutrophilic   |
|-----------|--------------------------------------|---|-------------------------------|----------------------------------|------------------------------|
| PC_O-34-2 | ns                                   | ** (R2 - 0.6396) (r - 0.7977)                     | * (R2 - 0.5444) (r - 0.7378)  | ** (R2 - 0.2691) (r - 0.5187)    | ns                           |
| PC_O-34-3 | * (R2 - 0.5947) (r - 0.7712)         | * (R2 - 0.4167) (r - 0.6455)                      | * (R2 - 0.5598) (r - 0.7482)  | ** (R2 - 0.3417) (r - 0.5846)    | ns                           |
| Ile       | ns                                   | ns  | ns                            | ns                               | * (R2 - 0.6378) (r - 0.7986) |
| PC_O-38-4 | * (R2 - 0.6055) (r - 0.7781)         | ns  | ** (R2 - 0.6035) (r - 0.7769) | ns                               | * (R2 - 0.2794) (r - 0.5286) |
| PC_38-4   | * (R2 - 0.5715) (r - 0.7559)         | * (R2 - 0.4094) (r - 0.6398)                      | * (R2 - 0.5799) (r - 0.7615)  | ns                               | * (R2 - 0.2812) (r - 0.5303) |
| CO        | ns                                   | ns  | ns                            | * (R2 - 0.6151) (r - 0.7843)     | ns                           |
| PC_38-6   | ns                                   | * (R2 - 0.4648) (r - 0.6818)                      | ns                            | * (R2 - 0.6145) (r - 0.7639)     | ns                           |

**Figure 6: Representative correlation plots between candidate metabolomic biomarkers for lung-DEARE and survival.** Representative examples of correlation plots from **Table 5** which lists significant metabolites and their Pearson's correlation (r) with survival. Data used for correlative analysis was from plasma analysis of AXR23, n=20; AXR24, n=38 (10 Gy PBI/BM5 (AXR23) or 10 Gy PBI/BM2.5 (AXR24)).

**Table 6. Correlation between candidate metabolomic biomarkers for lung-DEARE and histological scoring.** List of significant plasma metabolites illustrating their Pearson's correlation (r) with histological score. Correlation coefficient (R2) is also shown. Biomarker data used for correlative analysis was from plasma from AXR23/AXR24 (10 Gy PBI/BM5 (AXR23) or 10 Gy PBI/BM2.5 (AXR24)).

## ACKNOWLEDGEMENTS

### FUNDING:

This work was supported by NIAID contracts HHSN272201000046C (MacVittie, UMB); HHSN2722015000131 and 75N93020D00011 (Chang, SRI). Additional support was provided by the University of Maryland School of Pharmacy Mass Spectrometry Center (Kane, SOP1841-IQB2014).

COI: The authors declare no conflict of interest.

## REFERENCES

- MacVittie, Bennett, Health Phys. 2012; 103, 427-53 PMID: 22929471
- MacVittie, Farese, Health Phys. 2012; 103, 411-26. PMID: 22929470
- Farese, Bennett, Health Phys. 2019; 116, 339-353 PMID: 30281533
- MacVittie, Farese, Health Phys. 2019; 116, 305-338 PMID: 30542553
- Parker, GA Histopathology Atlas of Acute Radiation Syndrome and Delayed Effects in Rhesus Macaques. Academic Press, Elsevier, 2022. ISBN: 978-0-323-91393-5. <https://www.elsevier.com/books-and-journals>
- Kumar et al. Health Phys. 2020; 119, 594-603. PMID: 32347487
- Jones et al. Health Phys. 2019; 116, 473-483. PMID: 30624349
- Jones et al. Pharm Res. 2017; 34:2698-2709. PMID: 28971289
- Jones et al. Health Phys. 2019 Apr; 116:484-502. PMID: 30681425
- Zalesak-Kroves, Health Phys. 2021; 121:352-371. PMID: 34546217
- Jones JW et al. Anal Bioanal Chem. 2014, 406, 4663-75. PMID: 24842404
- Jones et al. Health Phys. 2015; 109: 452-65. PMID: 26425905
- Jones et al. Health Phys. 2015; 109: 440-51. PMID: 26425904
- Upcoming relevant publications in special issue of Health Physics: 14. Pandey & Kane, et al. Longitudinal plasma metabolomics after partial body irradiation in nonhuman primate reveals metabolomic signatures for acute radiation syndrome and delayed effects of acute radiation exposure. 2023, in preparation. 15. Pandey & Kane, et al. Plasma biomarkers in NHP that correlate with survival. 2023, in preparation. 16. Pandey & Kane, et al. Correlation with biomarker candidate for lung-DEARE with histological endpoints. 2023, in preparation. 17. Tudor Booth, et al. A quantitative histopathological characterization of the intestinal mucosa in the non-human primate (rhesus macaque). Part 1. Baseline. 2023, in preparation. 18. Tudor Booth, et al. A quantitative histopathological characterization of the intestinal mucosa in the non-human primate (rhesus macaque). Part 2. The Acute Radiation Response. 2023, in preparation. 19. Tudor Booth, et al. A quantitative histopathological characterization of the intestinal mucosa in the non-human primate (rhesus macaque). Part 3. The Delayed Effects of Acute Radiation Syndrome. 2023, in preparation.

